11th World Congress on Computational Mechanics (WCCM XI)
5th European Conference on Computational Mechanics (ECCM V)
6th European Conference on Computational Fluid Dynamics (ECFD VI)
E. Oñate, J. Oliver and A. Huerta (Eds)

NUMERICAL SIMULATION OF THE SOLIDIFICATION OF THE MELTED METAL BY THE PARTICLE METHOD

MASAKI KAZAMA* AND TAMON SUWA†

* Next Generation Technical Computing Unit, Fujitsu Limited
1-1, Kamikodanaka 4-chome, Nakahara-ku, Kawasaki 211-8588, JAPAN,
e-mail: kazama.masaki@jp.fujitsu.com

† Next Generation Technical Computing Unit, Fujitsu Limited
1-1, Kamikodanaka 4-chome, Nakahara-ku, Kawasaki 211-8588, JAPAN,
e-mail: suwa.tamon@jp.fujitsu.com

Key words: Casting process, Particle method, Solidification

Abstract. Particle methods such as the Smoothed Particle Hydrodynamics (SPH) method are computational methods that do not require a numerical mesh. As such, they are suitable for the numerical simulation of the semi-solid casting process, which is a kind of casting process. However, there are few precedent that the semi-solid casting was calculated by the particle method. We have developed the computational model of the shrinkage, the surface tension and the heat transfer. These are important elements to represent the semi-solid casting process. We show numerical results of the casting process by our method.

1 INTRODUCTION

In the casting process, we would like to get the casting of the objective shape by cooling the molten metal after having filled the mold with it. In order to reproduce the casting process by numerical computation, it is necessary to simulate the shrinking process of the molten metal by the solidification in addition to the flow and the heat transfer. We report a particle-based numerical model of the casting process which include the processes mentioned above.

In the casting simulation, the study of mesh-based methods such as the finite element method or the finite difference method are advanced. However, as for the mesh-based method, treating of the moving boundary, which is needed to calculate the interaction between moving mold and molten metal, is complicated. In the semi-solid casting, we push solidifying molten metal with the mold in order to fill that into the narrow space(Fig 1). Therefore the mesh-based methods are weak in the simulation of the semi-solid casting.

On the other hand, particle methods are suitable for the simulation of the semi-solid casting because treating of the moving boundary is relatively easy for the particle methods.

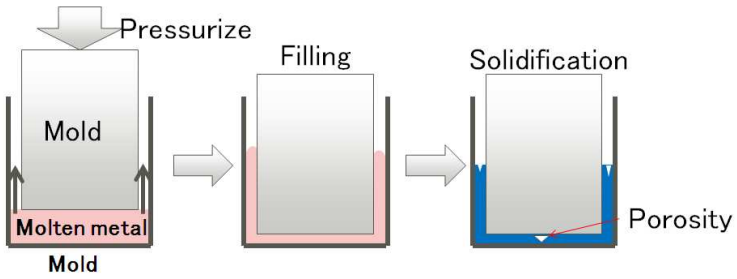

Figure 1: Example of the semi-solid casting

Cleary([1]) reported a particle-based numerical model of the casting process, which can be applied to low pressure die casting. They expressed the solidification and the shrinking as changes depending on temperature of the viscosity and the density, respectively. In their results, the shrinkage cavity and the residual pressure distributions in final castings are shown. These results imply possibility of the casting simulation by the particle method. However, the important elements in the calculation of semi-solid casting, which are mentioned later, were not introduced in their method. Then, in this study, we developed the numerical method based on that of Cleary for the semi-solid casting by the particle method.
When molten metal flows into the narrow space, the influence of the surface tension should not be ignored in the semi-solid casting. Moreover, when we calculate the pressurized fluid by the particle method, unnatural vibration of the density may become the problem. Therefore we enabled the numerical simulation of the semi-solid casting by introducing the numerical method controlling density vibration([2][3]), and the numerical model of the surface tension to the original method of Cleary.

2 SMOOTHED PARTICLE HYDRODYNAMICS

In this study, we apply Smoothed Particle Hydrodynamics(SPH) method, which is a particle method, to the casting simulation. The fluid equations are discretized by SPH as follows.

$$\frac{\mathrm{d}\rho_i}{\mathrm{d}t} = 2\rho_i \sum_j \frac{m_j}{\rho_j}(\boldsymbol{v}_i - \boldsymbol{v}_{ij}) \cdot \frac{\partial W(|\boldsymbol{x}_i - \boldsymbol{x}_j|, h)}{\partial \boldsymbol{x}_i}, \tag{1}$$

$$m_i \frac{\mathrm{d}\boldsymbol{v}_i}{\mathrm{d}t} = -2 \sum_j m_i m_j \left(\frac{p_{ij}}{\rho_i \rho_j} - \Pi_{ij} \right) \frac{\partial W(|\boldsymbol{x}_i - \boldsymbol{x}_j|, h)}{\partial \boldsymbol{x}_i}, \tag{2}$$

$$p_i = c^2(\rho_i - \rho_{s,i}). \tag{3}$$

Where, (1), (2), (3) express mass conservation law, momentum conservation law, and the equation of state, respectively. $m_i, \rho_i, \boldsymbol{v}_i, \boldsymbol{x}_i$, and p_i are the mass, the density, the velocity, the position and the pressure of i-th particle. c is the sound speed. Second term of the right hand side of (2) is the viscous stress term. When μ_i is the viscosity of the i-th particle, Π_{ij} is calculated as follows.

$$\Pi_{ij} = \frac{4m_j}{\rho_i \rho_j} \frac{\mu_i \mu_j}{\mu_i + \mu_j} (\boldsymbol{v}_i - \boldsymbol{v}_j) \cdot \frac{(\boldsymbol{x}_i - \boldsymbol{x}_j)}{|\boldsymbol{x}_i - \boldsymbol{x}_j|^2}. \tag{4}$$

Standard density $\rho_{s,i}$ is the density when the pressure of i-th particle becomes 0. W is a kernel function of SPH. In this work we use following form.

$$W(r,h) = \begin{cases} \alpha_d \left(1 - \frac{r}{h}\right)^4 \left(\frac{4r}{h} + 1\right) & (0 \leq r \leq h), \\ 0 & (h < r). \end{cases} \tag{5}$$

where α_d is set so that $\int W(|\boldsymbol{x}|, h) d\boldsymbol{x} = 1$ is satisfied. h is so-called the influence radius since the value of the kernel function becomes 0 outside the radius h. $p_{ij}, \boldsymbol{v}_{ij}$ are the pressure and the velocity calculated by the Reimann solver, respectively[2]. In addition, we apply normalization method to the calculation of the gradient of the kernel function[3].

To compare standard SPH method [4] with the SPH method using the Reimann solver, we show the following numerical results. We divided the fluid of the volume $1.12 \times 10^{-4} [m^3]$ into 57,399 particles and set $h = 0.00375[m]$, $c = 50[m/s]$, $m_i = 4.6875 \times 10^{-6}[kg]$, $\rho_{i,s} = 2400[kg/m^3]$. The initial condition of this simulation is the situation that the fluid is flowing into the cylinder at speed $1[m/s]$(Fig. 2).

Fig.3 indicates the density distribution of all particles at 0.08[s]. In standard SPH calculation, the density of all particles is in between $2200[kg/m^3]$ and $2650[kg/m^3]$, by contrast, in the simulation of SPH using the Reimann solver the density of all particles is in between $2392[kg/m^3]$ and $2408[kg/m^3]$. It is shown that the density vibration can be controlled by using the Riemann solver.

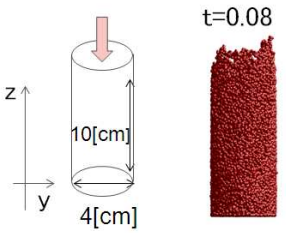

Figure 2: Setting of the filling simulation

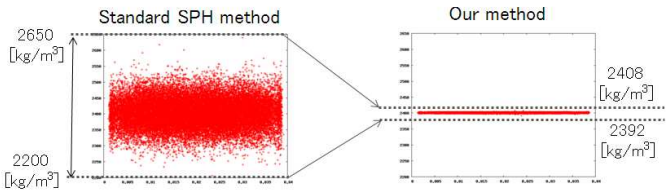

Figure 3: Density distribution of all particles

3 A NUMERICAL MODEL OF SURFACE TENSION

In SPH method, Continuum Surface Force(CSF) model that was expanded to be applicable to the particle method is known to calculate surface tension[5][6]. When we applied

CSF model to the simulation of the phenomenon that the water droplet collides to the wall, the calculation became unstable with unnatural vibration. Therefore, we developed the new numerical model of the surface tension based on the surface energy. In this section, we explain our model.

3.1 Surface energy

The droplet shape is studied based on the surface energy well[7].
Here, we define the following surface energy.

$$E_s = \int \Gamma_g \chi_{l>0} dS + \int \left[\Gamma_{sl} - \Gamma_{sg}\right] (1 - \chi_{l>0})\, dS. \tag{6}$$

The integration of (6) is calculated in whole surface of the fluid. l is the distance between the point on the fluid surface and the solid surface, and $\chi_{l>0}$ is the discontinuous function. If $l \leq 0$ is satisfied, the value of $\chi_{l>0}$ is 0, otherwise $\chi_{l>0} = 1$. Thus, the first term of the right hand side of (6) is the surface integral of the fluid surface contacting with the gas, and, the second term is the surface integral of the fluid surface contacting with the solid. Where, Γ_g, Γ_{sl}, Γ_{sg} are the surface tension coefficient of the fluid surface contacting with the gas, that of the fluid surface contacting with the solid and that of the solid surface contacting with the gas, respectively.
It is expected that the stationary point of the surface energy (6) under the volume preservation condition express the shape of the static droplet[8]. Then the contact angle θ satisfies $\cos\theta = -\frac{\Gamma_s}{\Gamma_g}$ (Fig.4). Where, $\Gamma_s = \Gamma_{sl} - \Gamma_{sg}$.

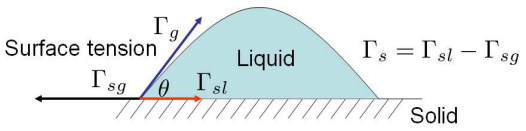

Figure 4: The surface tension and the contact angle

Furthermore, numerical results of the contact angle of the static soap bubble when $\theta < \frac{\pi}{2}$ is satisfied were shown by the finite element method[9].

3.2 An expression of the surface tension by SPH

Our model of the surface tension of the SPH method is constructed based on the surface energy.
First, we define the rate of granularity of the particle i as follow.

$$s_i = \sum_j \frac{m_j}{\rho_j} W(|\boldsymbol{x}_i - \boldsymbol{x}_j|, h). \tag{7}$$

The value of s_i is around 1 when particle i is in the fluid inside. By contrast, the value of s_i bacomes small when particle i is in the neighborhood of the fluid surface (Fig.5). As the next step, we define the following surface energy of SPH method by using s_i.

$$E_{s,p} = \sum_i g(1-s_i, 1-s_{min,i}) \left[\Gamma_g \tilde{\chi}(l_i,\epsilon) + \Gamma_s \left(1-\tilde{\chi}(l_i,\epsilon)\right)\right] \left(\frac{m_i}{\rho_i}\right)^{1-\frac{1}{d}}. \tag{8}$$

Where, d is the number of the space dimension. $\tilde{\chi}(l,\epsilon)$ is a smoothed expression of $\chi_{l>0}$ satisfying

$$\tilde{\chi}(l,\epsilon) = \begin{cases} 1 & (\epsilon \le l), \\ 3\left(\frac{l}{\epsilon}\right)^2 - 2\left(\frac{l}{\epsilon}\right)^3 & (0 \le l < \epsilon), \\ 0 & (l < 0), \end{cases} \tag{9}$$

and l_i is the distance between particle i and the solid surface. Typically $\epsilon = h$ is assumed.

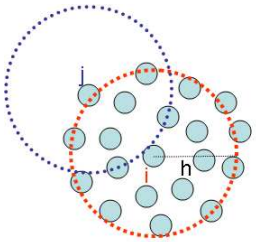

Figure 5: s_i bacomes small on the surface

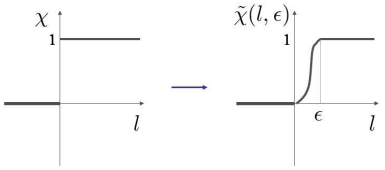

Figure 6: Smoothing function $\tilde{\chi}$

Multiplying the $\tilde{\chi}$ by surface tension coefficient expresses that the surface tension of i-th particle varies from Γ_g to Γ_s when the i-th particle approaches the solid surface. In order to calculate the summation of (8) only with particles near the surface, we introduce the function $g(1-s_i, 1-s_{min,i})$ satisfying

$$g(p,q) = R_d \begin{cases} p - \frac{q}{2} & (q \le p), \\ p\left(\frac{p}{q}\right)^2 - \frac{p}{2}\left(\frac{p}{q}\right)^3 & (0 \le p < q), \\ 0 & (p < 0), \end{cases} \tag{10}$$

where $s_{min,i} = \frac{m_i}{\rho_i} W(0,h)$ is the minimum of s_i. Since the value of s_i is around 1, i.e., p is around 0, when i-th particle is in fluid inside, $g(1-s_i, 1-s_{min,i})$ becomes 0 except in the case that i-th particle is near the surface. Therefore, the i-th particles which is in fluid inside do not contribute to the summation of the equation (8). Then, it is expected that $\left(\frac{m_i}{\rho_i}\right)^{1-\frac{1}{d}}$ express the surface area of the particle i, thus we are able to consider that

$$A_i = g_i \left(\frac{m_i}{\rho_i}\right)^{1-\frac{1}{d}}, \tag{11}$$

is proportional to the area of the surface of i-th particle exposed to outside. Moreover, we multiply R_d by A_i to express the surface area. R_d may depend on the number of the space dimension. R_d can be fixed by the vibration period of the surface tension wave. As a result of above-mentioned consideration, we get the following surface tension force to be added to particle i by using the surface energy (8).

$$\boldsymbol{f}_{s,i} = -\frac{\partial E_{s,p}}{\partial \boldsymbol{x}_i}. \tag{12}$$

We are able to introduce the effect of the surface tension by adding $\boldsymbol{f}_{s,i}$ to Eq. (2).
In two dimensional case, R_2 can be fixed by the numerical calculation of the solution of the surface tension wave. For example, the vibration solution is provided for the square fluid. Actually the vibration period is to be $0.4[s]$, when we assume that the fluid density $\rho = 798[kg/m^3]$, surface tsnsion coefficient $\Gamma_g = 23.61 \times 10^{-3}[N/m]$, initiai area is equal to $3.75 \times 10^{-2}[m^2]$ [10]. We divided the fluid into 4225 particles, and performed numerical simulation for the vibration of the surface tension by our method. The parameters were fixed as follows : $h = 1.76 \times 10^{-3}[m]$, $c = 1.76 \times 10^{-3}[m]$, $R_2 = 41.4$. Fig.7-Fig.9 show numerical results.

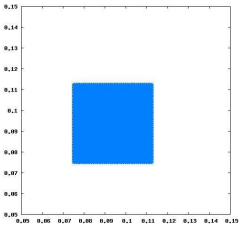

Figure 7: $t = 0.0[s]$

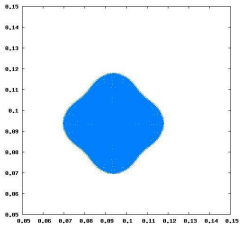

Figure 8: $t = 0.2[s]$

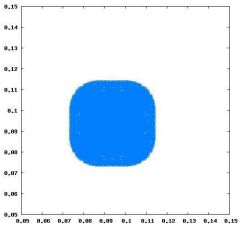

Figure 9: $t = 0.4[s]$

Since the shape of the fluid at $t = 0.4[s]$ is almost similar to the initial shape, we can choose correct value of R_2.

4 THE HEAT TRANSFER AND THE SOLIDIFICATION

In the casting, we should consider the following four processes of the heat transfer : (1) Heat conduction, (2) Heat transfer between the mold and the molten metal, (3) Heat transfer between the atmosphere and the materials and (4) Heat radiation.

In this section, we shall explain numerical models of four heat transfer processes. We also introduce numerical models of the solidification by Cleary.

4.1 Heat conduction

In the SPH method, the heat increment by heat conduction is calculated as follows [4].

$$Q_{hc,i} = -\sum_j \frac{4m_j}{\rho_j} \frac{\kappa_i \kappa_j}{\kappa_i + \kappa_j} (T_i - T_j) \frac{\partial W(|\boldsymbol{x}_i - \boldsymbol{x}_j|, h)}{\partial \boldsymbol{x}_i} \tag{13}$$

Where, $Q_{hc,i}$ is the heat increment per unit volume of particle i by the heat conduction. κ_i, κ_j are the heat conduction coefficient of particle i and particle j, respectively. T_i, T_j are the temperature of particle i and particle j.

4.2 Heat transfer between the mold and the molten metal

The heat increment by heat transfer from other object is calculated by the following numerical model.

$$Q_{ht,i} = -2h^2\pi\frac{\rho_i}{m_i}\sum_k \omega_{ik}\left(\frac{m_i}{\rho_i}+\frac{m_k}{\rho_k}\right)(T_i - T_k)W(|\boldsymbol{x}_i - \boldsymbol{x}_k|, h), \tag{14}$$

where ω_{ik} is the coefficient of heat transfer between particle i and particle k. We call $\sum_k \frac{1}{2}\left(\frac{m_i}{\rho_i}+\frac{m_k}{\rho_k}\right)W(|\boldsymbol{x}_i - \boldsymbol{x}_k|, h)$ the rate of granularity of k-th particles in radius h from i-th particle, since the value of this form nears 1 when enough number of k-th particles are in radius h from i-th particle. Thus, $2h^2\pi\frac{\rho_i}{m_i}\sum_k \left(\frac{m_i}{\rho_i}+\frac{m_k}{\rho_k}\right)W(|\boldsymbol{x}_i - \boldsymbol{x}_k|, h)$ is the value of multipying the surface area $4h^2\pi$ by the rate of granularity of the k particles in radius h around the particle i. Consequently, eq.(14) indicate Newton's law of cooling, because $Q_{ht,i}$ is proportional to the area contacting between particle i and particle k and the temperature difference between particle i and particle k.

4.3 Heat transfer between the atmosphere and the materials

We assume that the heat increment by the heat transfer between the atmosphere and the materials is proportional to the area of the surface exposed to outside and the temperature difference from the atmosphere. The exposed surface area is calculated by Eq.(11) which is defined in section 3.2. When the temperature of the atmoshere is expressed T_{atm}, the heat increment by the heat transfer between the atmosphere and the materials is calculated as follows.

$$Q_{ha,i} = -\frac{\rho_i}{m_i}\omega_{a,i}A_i(T_i - T_{atm}). \tag{15}$$

where, $\omega_{a,i}$ is the coefficient of heat transfer between the atmosphere and particle i.

4.4 Heat radiation

We apply the Stefan-Boltzmann law to the numerical method of the heat radiation. Since it is assumed that the heat increment by the heat radiation is proportional to the fourth power of the temperature and the exposed surface area of the particle, the heat increment by the heat radiation is calculated as follows.

$$Q_{hr,i} = -\frac{\rho_i}{m_i}\beta\sigma A_i(T_i - T_{atm})^4, \tag{16}$$

where β is emissivity, σ is the Stefan-Boltzmann constant.

4.5 The model of solidification

We employ the internal energy to express the latent heat by solidification. The latent heat can be expressed by taking the domain without the temperature change even if internal energy changes (Fig.10). The equation of the heat transfer process is as follows.

$$\rho_i \frac{\mathrm{d}u_i}{\mathrm{d}t} = Q_{hc,i} + Q_{ht,i} + Q_{ha,i} + Q_{hr,i}, \tag{17}$$

where, u_i is the internal energy per unit volume of particle i. In addition, the solidification and the shrinking can be expressed as changes depending on temperature of the viscosity and the density, respectively [1] (Fig.11).

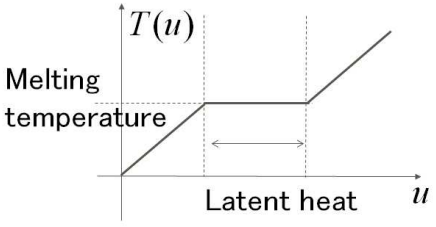

Figure 10: The example of the relationship between the internal energy and the temperature

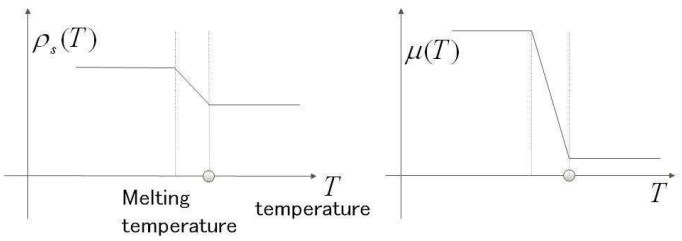

Figure 11: Solidification and shrinkage by SPH

5 NUMERICAL RESULTS

In order to perform simulation of the casting, we solve numerically eqs.(1)-(3) and (17). In this section, we shall show some numerical results by our method.

5.1 Conical molding

In this subsection, we show numerical results of conical molding. Conical molding is a method that is used for checking the feature of the shrinkage cavity of the molten metal easily[11]. The left-hand of Fig.12 shows a shape of the conical mold. The right-hand of Fig.12 is the initial position of particles for SPH simulation. The following parameters are used as the initial condition of this simulation. The standard density $\rho_{s,i} = 2398.8[kg/m^3]$, sound speed $c = 50[m/s]$, influence radius $h = 0.0045[m]$, mass of i-th particle $m_i = 8.10 \times 10^{-5}[kg]$, initial density of i-th particle $\rho_i = 2398.8[kg/m^3]$, initial temperature of i-th particle $T_i = 970[K]$. We started calculation with the situation that 95625 particles are filled in conical mold. In the right-hand of Fig.12, the red particles are the fluid particle and the yellow particles express the boundary of the conical mold. We constructed the physical properties of the molten metal by using the properties of AC4CH, which is an aluminum alloy. The Table 1 expresses the temperature dependence of the physical properties. u, T, μ, ρ_s and κ are the internal energy, the temperature, the

viscosity and the heat conduction coefficient, respectively. Γ_g is the surface tension of the surface contacted with gas. Then we assume the degree of wetting of the mold is perfectly non-wetting, so that Γ_s which is the parameter necessary to express the contact angle is set to Γ_g, i.e. $cos\theta = -1$. The parameter R_3 necessary for the calculation of the surface tension is set to 41.3.

Table 1: The Physical parameter of the molten metal(AC4CH)

$u[J/kg]$	$T[K]$	$\mu[m^2/s]$	$\rho_s[kg/m^3]$	$\kappa[W/m/K]$	$\Gamma_g[N/m]$
7.89×10^5	803.0	4.88×10^4	2571.9	174.35	0
8.44×10^5	830.44	4.73×10^4	2565.5	175.34	0
1.11×10^6	848	2.154×10^3	2517	114.78	0.932
1.23×10^6	873	1.86×10^2	2474.3	98.33	0.93
1.33×10^6	888.64	1.57×10^{-3}	2426.6	83.3	0.92
1.431×10^6	973	1.28×10^{-3}	2398.8	86.05	0.89

The molten metal begins to solidify from $T = 888.64[K]$, then the solidification is finished when the temperature of the molten metal falls less than $830.44[K]$. The latent heat is expressed by changing dramatically the internal energy when the temperature varies from $888.64[K]$ to $830.44[K]$.
The temperature of molten metal on the mold surface is fixed $300[K]$, since the molten metal is cooled uniformly by the mold. Then we calculate the cooling process by the heat conduction model.

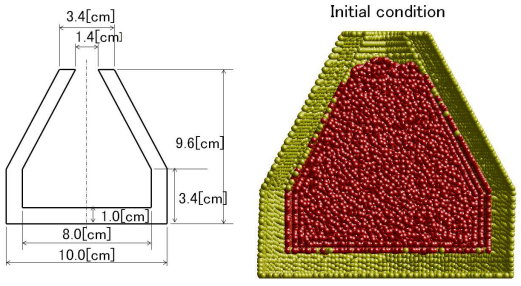

Figure 12: The shape of the mold and the initial condition of numerical simulation

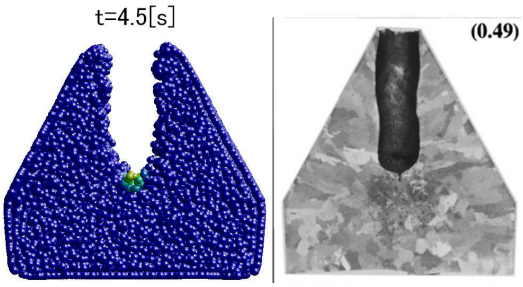

Figure 13: Shrinkage cavity

The left-hand of Fig.13 shows the shape of the solidification metal which is obtained by slicing off the numerical result of the center part to $0.009[mm]$ of thickness. The right-hand of Fig.13 shows the shape of the casting of AC4CH which is obtained by the experiment[11]. We can compare the experimental result and numerical result in terms of the shape of the shrinkage cavity. The numerical result is similarly to the experimental result.

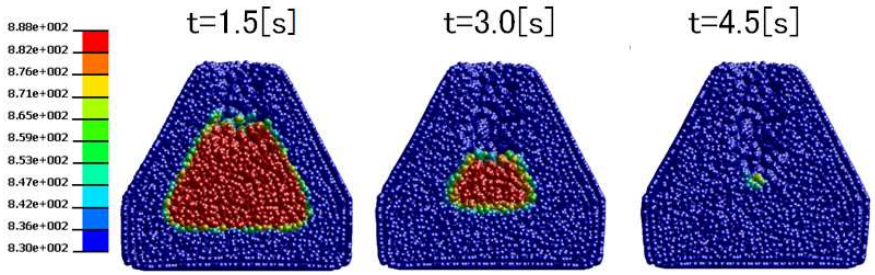

Figure 14: The cooling process

Fig.14 shows the cooling process. The red particles are the particles the temperature of which is more than $888[K]$. The temperature of the blue particles are less than $830[K]$. These results also shows the position which is solidified at the end.

5.2 Semi-solid casting

We performed numerical calculation of an injection process using AC4CH as an example of the semi-solid casting. The shape of the mold to pour molten metal has the ditch of the cross midmost, as shown in Fig.15. Fig.16 explains the diagram of the casting method. In this case, we started pushing of the upper mold the mass of which is $800[g]$ after $0.2[s]$ later pouring molten metal into lower mold. Then we mold molten metal into the casting of thickness $1.5[mm]$. The initial parameters of particles which express the molten metal are set as follows. The mass of i-th particle $m_i = 1.012 \times 10^{-6}[kg]$, initial density $\rho_i = 2398.8[kg/m^3]$, standard density $\rho_{s,i} = 2398.8[kg/m^3]$, the influence radius $h = 0.00225[m]$, initial temperature is $970[K]$ and the sound speed $c = 50[m/s]$. We use 232570 particles to express the molten metal. Moreover, we apply Table 1 to the temperature dependence of the physical properties of the molten metal.

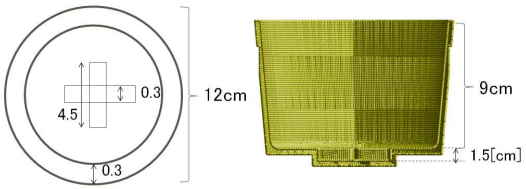

Figure 15: Shape of cast

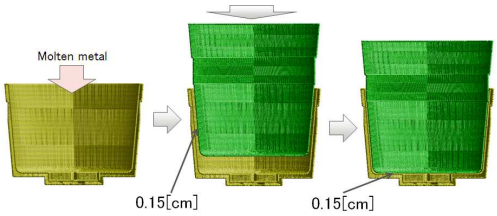

Figure 16: The diagram of cast

We used physical properties of iron as the properties of the mold, that is, density, heat conductivity and the emissivity are $7874[kg/m^3]$, $26.0[W/m/K]$ and 0.3, respectively. The specific heat is $800[J/kg/K]$ when temperature is $973.15[K]$, it is $640[J/kg/K]$ when temperature is $773.15[K]$. In this calculation we assumed that the heat radiation and

the heat transfer between the molten metal and the atmosphere can be ignored, since the molten metal is surrounded by the mold. Therefore we consider the heat conduction of the mold and the molten metal, the heat transfer between the molten metal and the mold, between the mold and the atmosphere and the heat radiation of the mold as the heat transfer process. The temperature of the atmosphere is fixed $300[K]$, then we fix the value of the coefficient of the heat transfer between the molten metal and the mold at $150[W/m^2/K]$, and the value of the coefficient of the heat transfer between the mold and the atmosphere at $80[W/m^2/K]$. These coefficients are fixed so that solidification time of simulation is correspond to the experimental one.

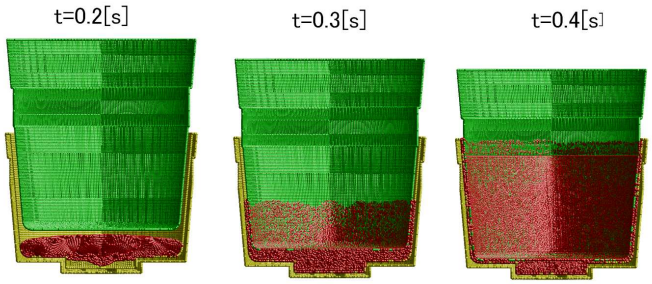

Figure 17: Press the molten metal

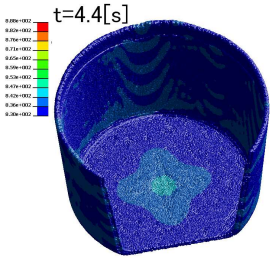

Figure 18: solidification

Fig.17 shows the numerical results while pushing the molten metal by the upper mold. The molten metal flows into the narrow space between the upper mold and the lower mold. Fig.18 shows the shape of the casting which have been almost solidified. It is expected that the region of the ditch of the cross is solidified at the end.

6 CONCLUSIONS

In this work, we introduced the numerical model of the surface tension and heat transfer processes involving heat radiation to the method of Cleary. Furthermore, we applied the Riemann solver to estimation of pressure and velocity in the momentum equation of SPH. As a result, we are able to calculate the flow and solidification of the molten metal at the same time while controlling density vibration by our method. The shape of shrinkage cavity of the numerical results of the conical molding are similar to the experimental results. We also performed the numerical calculation of the semi-solid casting, which is difficult for numerical methods using the mesh. These results represent the possibility that our method is applicable to the simulation of the semi-solid casting. We are going to compare with the experiment of the semi-solid casting in future.

REFERENCES

[1] Paul W. Cleary. Extension of SPH to predict feeding freezing and defect creation in low pressure die casting, *Applied Mathematical Modelling*, (2010)Vol. **34**:3189–3201.

[2] S. Inutsuka, Reformulation of Smoothed Particle Hydrodynamics with Riemann Solver, *Journal of Computational Physics*,(2002) Vol. **179**:238–267.

[3] G. Oger, and M. Doring, B. Alessandrini, P. Ferrant, An improved SPH method: Towards higher order convergence, *Journal of Computational Physics*,(2007) Vol. **225**:1472–1492.

[4] Monaghan J.J., Smoothed Particle Hydrodynamics, *Annu. Rev. Astrn. Astrophys.*,(1992) Vol.**30**:543–573.

[5] B. Lafaurie, C. Nardone, R. Scardovelli, S. Zaleski, and G. Zanetti, Modelling Merging and Fragmentation in Multiphase Flows with SuRFER, *Journal of Computational Physics*,(1994) Vol. **113**:134–147,

[6] X.Y. Hu, N.A. Adams,A multi-phase SPH method for macroscopic and mesoscopic flows, *Journal of Computational Physics*, (2006) **213**:844–861,

[7] Pierre-Gilles de Gennes, Francoise Brochard-Wyart, David Quere, *Capillarity and Wetting Phenomena: Drops, Bubbles, Pearls, Waves*. Springer (2003)

[8] K.Svadlenka, S.Omata,Construction of solutions to heat-type problems with volume constraint via the discrete Morse flow. *Funkcialaj Ekvacioj*,(2007) **50** No.2:261–285.

[9] T. Yamazaki, S. Omata, K. Svadlenka, K. Ohara: Construction of approximate solution to a hyperbolic free boundary problem with volume constraint and its numerical computation. *Advances in Mathematical Science and Applications*, (2006) **16**:57–67.

[10] J.U. Brackill, C. Zemach, A continuum method for modeling surface tension. *Journal of Computational Physics*, (1992) **100**:335–354.

[11] Y. AWANO, Shrinkage property of Al-Si casting alloys during solidification. *Journal of Japan Institute of Light Metals*, (2006),Vol.**56**,No.6:335–342.